

# Identified hadron production at SLD and BABAR

David Muller, on behalf of the SLD and BABAR Collaborations

Stanford Linear Accelerator Center, Stanford, California, USA

Received: 31 October 2003 / Accepted: 9 January 2004 /

Published Online: 19 February 2004 – © Springer-Verlag / Società Italiana di Fisica 2004

**Abstract.** We present measurements of identified hadron spectra in  $e^+e^- \rightarrow$  hadrons from the BABAR and SLD experiments at respective c.m. energies of 10.54 GeV and 91.2 GeV. The scaling violations between the two energies are found to be large and described by hadronization models for charged pions, but not for heavier hadrons. SLD measurements show large differences between  $b\bar{b}$ ,  $c\bar{c}$  and light-flavor events that are qualitatively consistent with expectations. The light flavor events are somewhat more consistent with the predictions of MLLA QCD than are events of all flavors, but a discrepancy in the mass dependence remains. SLD have made several new and/or improved measurements of light leading particle production, paving the way for future tagging of  $u$ ,  $d$  and  $s$  jets. They have also made a unique study of signed rapidity correlations, showing direct evidence for charge ordering of protons along the quark-antiquark axis.

## 1 Introduction

The process of hadronization, by which an energetic quark or gluon from a hard collision forms a jet of hadrons, remains a frontier in elementary particle physics. Quantitative QCD calculations are challenging, however some inclusive jet properties have been calculated in the Modified Leading Logarithm Approximation (MLLA) [1], the dependence of  $x_p = 2p/E_{CM}$  distributions on center-of-mass energy  $E_{CM}$  has been calculated at high  $x_p$  [2], and phenomenological models of hadronization have been developed [3,4,5]. Measurements of jet properties test these models and encourage theoretical development. Since jets are used in precision tests of electroweak and strong physics and will constitute the largest signal for, and background to, any heavy particles to be discovered, our understanding must be as complete as possible. The identification of specific jets as initiated by a  $q$  or  $\bar{q}$  of a particular flavor, or a gluon, would be especially useful.

The statistics available at the  $Z^0$  and the  $B$  factories enable precise measurements of inclusive jet properties over wide kinematic ranges. Detectors with advanced particle identification allow such measurements for individual particle species. In Sect. 2 we present spectra of  $\pi^\pm$ ,  $K^\pm$  and  $p/\bar{p}$  from SLD [6], and of  $\pi^\pm$ ,  $K^\pm$ ,  $p/\bar{p}$  and  $\eta$  from BABAR [7]; we compare with theoretical and model predictions, and study their energy dependence.

Modern vertex detectors allow the separation of light- and heavy-flavor events. In Sect. 3 we compare light ( $u\bar{u}$ ,  $d\bar{d}$  and  $s\bar{s}$ ),  $c\bar{c}$  and  $b\bar{b}$  events from SLD. Expanded studies of light leading particle production from SLD, through a combination of quark (vs. antiquark) jet tagging and long range rapidity correlations, are described in Sect. 4. Similar correlation studies at short range provide unique probes of the hadronization process, including a direct window on charge ordering, and are discussed in Sect. 5.

## 2 Inclusive identified particle spectra

The BABAR and SLD detectors feature state of the art charged hadron identification over a large fraction of the kinematic range. SLD uses a dual radiator ring-imaging Cherenkov device, and BaBar combines a novel internally reflecting Cherenkov imager with  $dE/dx$  measurements. The resulting measured spectra in hadronic events in Fig. 1 show excellent precision and coverage. BABAR also includes a precise CsI electromagnetic calorimeter to measure the energies of photons. They reconstruct  $\eta \rightarrow \gamma\gamma$  and the resulting spectrum, also shown in Fig. 1 has complete coverage and excellent precision.

SLD have compared their spectra with the predictions of the JETSET (J) [3], HERWIG (H) [4] and UCLA (U) [5] models, finding that all are able to describe the data qualitatively, but not in detail: the  $\pi^\pm$  spectrum is described within 2% except for  $x_p > 0.5$  where J (H) is (much) too high, and  $x_p < 0.02$  where H (U) is too high (low); the  $K^\pm$  spectrum is too high (low) in all models for  $x_p < 0.04$  and in H (J, U) for  $x_p > 0.5$ ; J describes the shape of the  $p\bar{p}$  spectrum, but is 10% too high at all  $x_p$ , whereas U and H describe the spectrum for  $x_p < 0.4$  but show structure inconsistent with the data at higher  $x_p$ .

BABAR have considered JETSET, UCLA, and a version of JETSET with modified parameters (M) that describes the  $p/\bar{p}$  and  $\pi^\pm$  spectra at the  $Z^0$ . They find a somewhat worse general description of the data at their lower energy: the  $\pi^\pm$  spectrum is described at low  $x_p$  and by M at high  $x_p$ , whereas the J and U are too high at intermediate  $x_p$  then fall low; the  $K^\pm$  spectrum shows similar features, and all models are also too high for  $x_p < 0.1$  and the M is high for  $x_p > 0.8$ ; the description of the  $p/\bar{p}$  spectrum is poor, with the J being high overall and especially at high  $x_p$ , M being slightly high at low  $x_p$  but very high at high  $x_p$ , and U being low (high) at low (high)  $x_p$ .

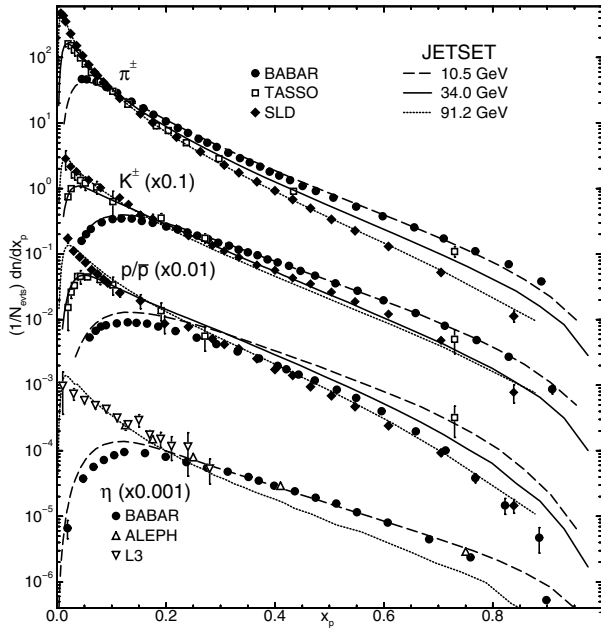


**Fig. 1.** Cross sections vs.  $x_p = 2p/E_{CM}$  from BaBar (dots), SLD (diamonds), and JETSET (lines). Also shown are data from TASSO at 34 GeV, and L3 and ALEPH at the  $Z^0$

The high precision at these two very different energies allows the precise study of scaling properties. This is shown in Fig. 1 for the data and the JETSET model, where we have included charged hadron data from TASSO at  $E_{CM}=34$  GeV and  $\eta$  data from L3 and ALEPH. In the case of  $\pi^\pm$ , the scaling violations at both high and low  $x_p$  are described by the model. However for  $K^\pm$  the model predicts a larger (smaller) shift than is seen in the data at high (low)  $x_p$  by as much as 30%. For  $p/\bar{p}$  and  $\eta$  this discrepancy is even larger; in particular there is very little difference in the data at high  $x_p$  whereas the model predicts a large difference. Similar results hold for the other models; this reduction in scaling violations with mass is a new challenge for their authors.

The predictions of MLLA QCD have been tested by transforming the measured cross sections to the variable  $\xi = -\ln x_p$  and fitting Gaussian and distorted Gaussian functions to the regions near their peaks. The data for each hadron can be described by a Gaussian within about one unit of the peak and with the addition of small skewness and kurtosis terms over a larger range, consistent with one prediction of MLLA. The peak positions  $\xi^*$  are different at the two energies, as expected, and the world's data are consistent with the predicted logarithmic dependence of  $\xi^*$  on  $E_{CM}$  for each particle, although the data at other energies have much larger uncertainties (there are none for  $\eta$ ). However the predicted exponential dependence on particle mass at a given  $E_{CM}$  is not seen at either energy; the values for  $K^\pm$  and  $\eta$  are substantially lower than those for the respective  $\pi^\pm$ , however those for  $p/\bar{p}$  are not lower than those for  $K^\pm$ . This is discussed further in the next section, along with total yields per event.

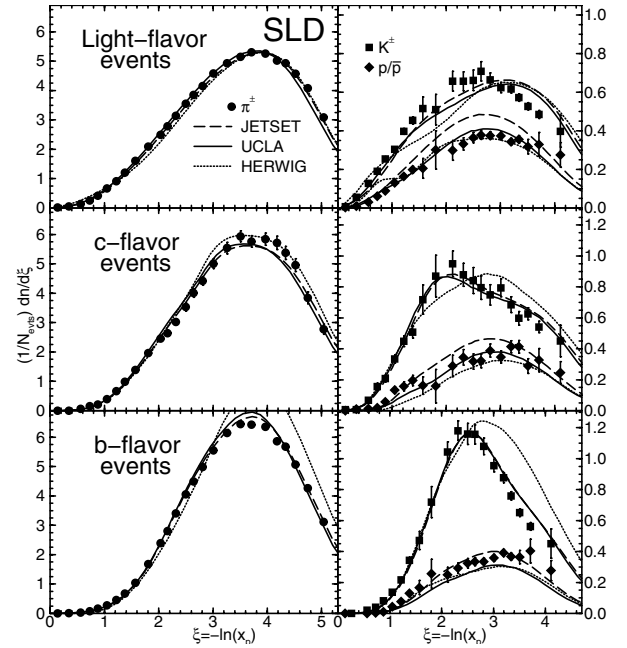


**Fig. 2.** Charged hadron cross-sections vs.  $\xi = -\ln x_p$  for light,  $c\bar{c}$  and  $b\bar{b}$  events, compared with model predictions

### 3 Flavor dependence

$Z^0 \rightarrow b\bar{b}$  ( $c\bar{c}$ ) events produce leading  $B$  ( $D$ ) hadrons with few mm flight distances, which can be used to (anti)tag  $b\bar{b}$  and  $c\bar{c}$  ( $u\bar{u} + d\bar{d} + s\bar{s}$ ) events for a variety of physics. SLD derives the  $\xi$  spectra in Fig. 2. The same model deficiencies are seen in light- as in all-flavor events; many are larger, particularly the structures at low  $\xi$  (high  $x_p$ ) in H. The spectra in  $b\bar{b}$  and  $c\bar{c}$  events are quite different, as expected. The models describe the  $\pi^\pm$  spectrum in  $c\bar{c}$  events reasonably well, J and U describe the  $K^\pm$  spectrum, and all describe the shape of the  $p/\bar{p}$  spectrum, except for a hint of structure at low  $\xi$ . All describe the shape of the  $p/\bar{p}$  spectrum in  $b\bar{b}$  events and the rising edge of the  $K^\pm$  and  $\pi^\pm$  spectra, but fail for  $\xi > 3$  units, especially H.

(Distorted) Gaussians can describe the data for light-flavors, and for heavy flavors in the peak regions, but very large distortion terms are needed to extend the range. MLLA uses massless partons and may not be applicable to  $b\bar{b}$  and  $c\bar{c}$  events, which are clearly affecting the overall spectra and  $\xi^*$ . Measurements of  $\xi^*$  at the  $Z^0$  are summarized in Fig. 3. The all-flavor measurements (left) do not show a monotonic mass dependence, although mesons and baryons may follow parallel trajectories. The light-flavor  $\xi^*$  (right) are closer to a single trajectory, however they remain inconsistent with the prediction.

BABAR obtains a total yield of  $0.235 \pm 0.012$   $\eta$  mesons per event; charged hadron results are given in Table 1. The uncertainties are generally dominated by overall tracking or photon finding efficiencies.  $c\bar{c}$  (and  $b\bar{b}$ ) events produce substantially more  $K^\pm$  (and  $\pi^\pm$ ) than light-flavor events; there is little difference in  $p/\bar{p}$  production.

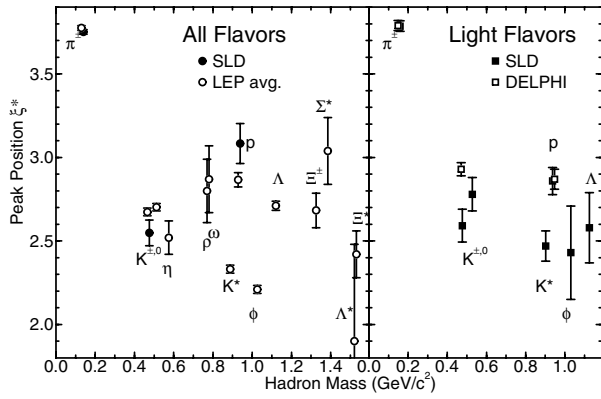


**Fig. 3.** Peak positions  $\xi^*$  in all- (left) and light- (right) flavor events at the  $Z^0$  as a function of hadron mass

**Table 1.** Yields of each hadron type in events of each flavor

	$\pi^\pm$	$K^\pm$	$p/\bar{p}$
BaBar	$6.405 \pm 0.172$	$0.910 \pm 0.018$	$0.276 \pm 0.017$
SLD All	$17.007 \pm 0.209$	$2.203 \pm 0.071$	$1.054 \pm 0.035$
<i>uds</i>	$16.579 \pm 0.304$	$2.000 \pm 0.068$	$1.094 \pm 0.043$
<i>c</i>	$16.954 \pm 0.556$	$2.427 \pm 0.100$	$1.034 \pm 0.077$
<i>b</i>	$18.136 \pm 0.330$	$2.510 \pm 0.086$	$1.004 \pm 0.046$
<i>b</i> - <i>uds</i>	$1.557 \pm 0.232$	$0.510 \pm 0.037$	$-0.091 \pm 0.074$
<i>c</i> - <i>uds</i>	$0.375 \pm 0.587$	$0.427 \pm 0.074$	$-0.060 \pm 0.034$
<i>b</i> - <i>c</i>	$1.182 \pm 0.498$	$0.083 \pm 0.075$	$-0.031 \pm 0.074$

## 4 Light leading particles and correlations

SLD use their  $e^-$  beam polarization to divide each light-tagged event into  $q$  and  $\bar{q}$  hemispheres (73% purity), and measure both  $\sigma_h$  and  $\sigma_{\bar{h}}$ ,  $h = \pi^-, K^-, p$ , in light  $q$  jets. Normalized differences  $D_h = (\sigma_h - \sigma_{\bar{h}})/(\sigma_h + \sigma_{\bar{h}})$  are shown in Fig. 4: the large positive  $D_p$  at high  $x_p$  signals leading proton production;  $D_{\pi^-}$  is smaller since  $d$  and  $\bar{u}$  jets contribute with opposite sign; the large  $D_{K^-}$  indicates leading kaons predominantly from  $s$  jets. The models describe  $D_{\pi^-}$  and  $D_{K^-}$ , but U and H are inconsistent with  $D_p$ .

Long-range correlations also probe leading hadrons. For  $p > 8$  GeV/c, excesses of opposite- over same-charge  $\pi\pi$ ,  $\pi p$ ,  $KK$  and  $pp$  pairs are seen [6] at high rapidity difference  $|\Delta y|$ , due to the leading hadrons from the  $q$  and  $\bar{q}$ . These sources of information can be combined by signing  $y > 0$  for tracks in the  $q$  hemisphere. A sample signed  $\Delta y_{KK}^{+-} = y_{K^+} - y_{K^-}$  distribution is shown in Fig. 5a. Excesses over randomly signed same-charge pairs are seen at large negative and positive values of  $\Delta y_{KK}^{+-}$ , dominated by  $s\bar{s}$  events and a mixture of flavors, respectively. Enough such measurements can yield the contributions from  $u$ -,  $d$ - and  $s$ -jets, leading to a light flavor tagging procedure.

Signed  $y$  give other new probes of hadronization, e.g. the  $y_p - y_{\bar{p}}$  distribution in Fig. 5b, which shows a shift to the positive side in the central peak. These are mostly locally correlated  $p\bar{p}$  pairs; the shift indicates that such pairs tend to align with the  $p$  ( $\bar{p}$ ) following the  $q$  ( $\bar{q}$ ) direction. The

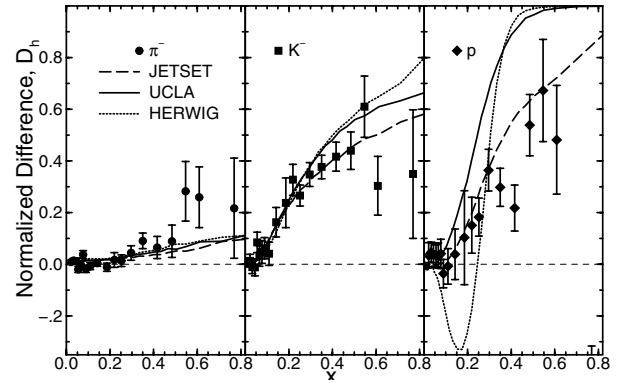


**Fig. 4.** Normalized differences between hadron and antihadron production in light quark (rather than antiquark) jets

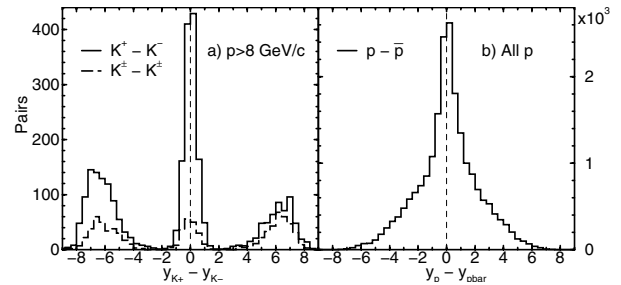


**Fig. 5.** Differences in signed rapidity for **a**  $KK$  pairs with  $p > 8$  GeV/c and **b** all  $p\bar{p}$  pairs

effect is present at all  $p$  and  $y$ , indicating baryon number ordering along the entire hadronization chain.

## 5 Summary

More  $e^+e^- \rightarrow$ hadrons data with modern detectors continue to give new insights into the hadronization process.  $K^\pm$ ,  $\eta$  and  $p/\bar{p}$  data from BABAR (10.54 GeV) and SLD (91.2 GeV) show much smaller scaling violations than expected. The primary  $q\bar{q}$  flavor affects event properties strongly; light-flavor data show larger problems in hadronization models, and better, though imperfect, agreement with MLLA QCD. The initial  $q$  and  $\bar{q}$  are “contained” in relatively energetic leading hadrons with those quark types as valence constituents. Improved understanding of leading hadrons will allow tagging of light jet flavors, as is common for  $b$  and  $c$ . A unique study of signed rapidities provides direct evidence for baryon number ordering along the entire hadronization chain.

## References

1. T.I. Azimov, Y.L. Dokshitzer, V.A. Khoze, and S.I. Troyan: *Z. Phys. C* **27**, 65 (1985)
2. See e.g. B.A. Kniehl, G. Kramer, and B. Pötter: *Nucl. Phys. B* **582**, 514 (2000)
3. T. Sjöstrand: *Comp. Phys. Comm.* **82**, 74 (1994)
4. G. Marchesini et al.: *Comp. Phys. Comm.* **67**, 465 (1992)
5. S. Chun and C. Buchanan: *Phys. Rep.* **292**, 239 (1998)
6. SLD Collab.: SLAC-PUB-9949, submitted to *Phys. Rev. D*
7. BaBar Collaboration: private communication